Submitted to J. Am. Cer. Soc.

Preparation of $K_{0.5}Na_{0.5}NbO_3$-based piezoelectrics by spray pyrolysis and challenges with sintering

Astri Bjørnetun Haugen, Francesco Madaro, Lars-Petter Bjørkeng, Jon Martinsen Strand, Tor Grande and Mari-Ann Einarsrud*

Department of Materials Science and Engineering, Norwegian University of Science and Technology, N-7030 Trondheim, Norway

*Corresponding author:

Mari-Ann Einarsrud

mari-ann.einarsrud@ntnu.no

phone: +47 48136521

fax: +47 73550203

Abstract

$K_{0.5}Na_{0.5}NbO_3$ (KNN)-based ceramics are promising lead-free piezoelectrics, but processing of these materials is an ongoing challenge. Here, we present a spray pyrolysis route to high-quality KNN-based powders. Fine-grained (<100 nm as-prepared, ~130 nm calcined at 800 °C) and phase-pure KNN and $Li_{0.03}K_{0.485}Na_{0.485}Nb_{0.8}Ta_{0.2}O_3$ (KNNLT) powders were obtained from aqueous precursor solutions. Ceramics with 95 % of theoretical density and with normalized strain of 333 pm/V were obtained by conventional sintering. The sintering of KNN remained challenging even for the fine grained powders, and the origins of these processing challenges were investigated by dilatometry and electron microscopy. Coarsening into cuboidal grains, which strongly reduced the sinterability, was observed in alkali-oxide excess KNN, caused by the formation of a liquid phase at ~650 °C. We propose that the reactivity of alkali oxide with moisture and carbon dioxide at lower temperatures cause the formation of the liquid phase at the surface even for stoichiometric KNN powders. Evaporation, mainly of potassium oxide, at high temperatures was shown to cause the formation of a Nb-rich secondary phase. The segregation of a secondary phase and inhomogeneous distribution of K/Na are discussed in relation to sintering above the solidus temperature of KNN.

Introduction

$K_{0.5}Na_{0.5}NbO_3$ (KNN) is one of the most studied lead-free piezoelectric material systems[1] which, by doping and texturing exhibit comparable properties to lead zirconate titanates.[2] The preparation of dense and stoichiometric KNN ceramics[3,4] has however been a persistent challenge due to the hygroscopic nature of alkali carbonate precursors,[5] volatility of alkali oxides[6-8] and narrow sintering interval close to the solidus temperature.[9-11] As denser ceramics typically yield improved piezoelectric coefficients, many have endeavored to improve performance through optimizing synthesis and sintering procedures. While conventionally air-sintered KNN typically reaches densities of 90-93 %[1] and d_{33} values of 80-120 pC/N,[4] increasing the density to above 99 % by hot pressing improves the d_{33} to 160 pC/N.[12] Dopants targeting to improve the sintering behavior have been extensively studied.[3] These sintering aids either introduce alkali (A-site) or oxygen vacancies, or liquid phase, lowering the sintering temperature and improve the degree of densification,[3] although sometimes at the sacrifice of piezoelectric performance.[13] Li and Ta doping are introduced mainly to improve the piezoelectric performance of KNN (d_{33} values of 220 pC/N[2] or 310 pm/V[14]), although Ta also improves the densification to some extent by reducing the rate of grain growth.[1]

As an alternative to doping, the stoichiometry of KNN can be modified as an attempt to improve sintering. Excess Nb (B-site) can be introduced in order to generate alkali vacancies in KNN[9,15] albeit at the risk of forming Nb-rich secondary phases.[15] Excess Nb is therefore considered an undesired consequence of alkali evaporation during sintering. The degree of evaporation is dependent on temperature, duration and atmosphere. KNN is typically sintered in an oxygen-rich atmosphere to avoid oxygen vacancies pinning domain motion,[16] yet it has also been demonstrated that sintering in a reducing atmosphere suppresses grain growth.[17]

Non-stoichiometric KNN with an alkali excess has also been prepared with the aim of creating a liquid phase to aid densification; however alkali excess is usually observed to cause exaggerated grain growth in the powder which reduces the sinterability.[5,15]

Synthesizing KNN using conventional solid state reaction techniques often requires excessive calcination temperature and duration, making alkali evaporation possible during calcination as well as sintering. Reducing the particle size of the precursors allows calcination at lower temperatures, but requires high-energy milling (e.g. mechanochemical activation[18]) which increases the risk of contamination. Both the water content in the hygroscopic alkali carbonate precursors and alkali evaporation during processing must be compensated for by the introduction of excess alkali.[15,19-22] Solid state processing of KNN (especially Li and Ta co-doped KNN) can also result in inhomogeneity unless a pre-reaction of the B-site oxides through the "precursor method" is performed.[23,24]

Wet chemical methods generally produce homogeneous ceramic powders of small particle size with good stoichiometry control. KNN-based powders have been prepared by hydrothermal,[25,26] spray drying[27,28] and sol-gel[22,29,30] syntheses among others, and high density and excellent piezoelectric properties have been obtained.[22] Spray pyrolysis[31] combines the high quality of powders from the wet chemical methods with possibility for large scale production. Aqueous (rather than organic) precursor solutions of nitrates provide additional practical, environmental and economic advantages.[32]

This work is motivated by previous success with the preparation of fine-grained oxide powders for functional materials by spray pyrolysis[33-35] and the challenges in processing of KNN by solid state methods. Here we report on the synthesis of fine-grained KNN and doped

KNN powders prepared by spray pyrolysis of aqueous solutions. The effect of cation non-stoichiometry and sintering conditions are investigated with focus on the effect on the phase composition and densification of the ceramics. The particular challenges related to the densification of KNN-based materials are discussed with emphasis on secondary liquid phases and possible reactions with CO_2/H_2O and loss of alkali oxides.

Experimental

I. Powder synthesis and sintering

$K_{0.5}Na_{0.5}NbO_3$ (KNN) and $Li_{0.03}K_{0.485}Na_{0.485}Nb_{0.8}Ta_{0.2}O_3$ (KNNLT) powders in batches up to 3 kg were synthesized by a pilot-scale spray pyrolysis equipment. Aqueous precursor solutions were prepared from KNO_3, $NaNO_3$ (>99%, Merck, Darmstadt, Germany), $LiNO_3$ (>99%, Sigma Aldrich, St Louis, MO), Ta-oxalate solution (H.C. Starck, Goslar, Germany) and ammonium niobium dioxalate oxide pentahydrate (H.C. Starck, Goslar, Germany) dissolved in distilled water. The alkali nitrates were dried at 200 °C, and Nb- and Ta-solutions thermogravimetrically standardized at 800 °C before stoichiometric quantities were mixed. The solutions were atomized through a two-phase nozzle into a tube furnace (~800 °C at the nozzle), where droplets of precursor solution dried into hollow, spherical soft agglomerates consisting of fine primary particles. The as-prepared powders were calcined for 6 h (KNNLT at 600 °C, KNN at 800 °C), milled and sieved through a 250 μm sieve. Non-stoichiometric KNN was produced by soaking calcined, stoichiometric KNN powder into KNO_3, $NaNO_3$ or ammonium niobium dioxalate oxide pentahydrate aqueous solutions, evaporating the water and performing a second calcination at 400 or 800 °C. Green bodies were prepared by uniaxially pressing at 130 MPa. A range of set temperatures (1100-1160 °C), heating rates (3.3 °C/min, 5 °C/min and >1100 °C/min), hold times (1-14 h) and atmospheres (air and O_2)

were investigated for isothermal sintering. The highest heating rate (>1100 °C/min) was obtained by inserting the green bodies into a preheated furnace.

II. Characterization of powders and sintered materials

The microstructures of powders and sintered materials were characterized by scanning electron microscopy (S-3400N and S-5500, Hitachi, Hitachi, Japan and Ultra 55, Carl Zeiss AG, Oberkochen, Germany). X-ray diffraction (XRD) patterns from Cu Kα radiation were recorded with a D8Focus diffractometer (Bruker AXS, Karlsruhe, Germany). Phase transitions in the temperature range 100-500 °C were studied by differential scanning calorimetry (DSC) (DSC 7, Perkin Elmer, Waltham, MA) with 60 °C/min heating and cooling rates. Using nitrogen absorption, the average particle size (assuming spherical particles) was determined through the BET method (TriStar 3000, Micromeritics, Norcross, GA). The pH of dispersions of KNN and non-stoichiometric KNN powders (~10 wt% powder in distilled water) was measured with universal pH-indicator strips. Each measurement was performed twice. Linear shrinkage during heating at 2 and 10 °C/min in synthetic air, O_2 and N_2 was studied with a dilatometer (DIL 402E, Netzsch, Selb, Germany). Densities of sintered materials were measured by the Archimedes' method using isopropanol (ISO 5017). Wavelength dispersive X-ray spectrometry (WDS) was performed with a JXA-8500F (JEOL, Tokyo, Japan) on polished surfaces. Piezo- and ferroelectric properties of Ag-electroded ceramics were investigated with a piezoelectric testing system (TF Analyzer 2000, aixACCT Systems GmbH, Aachen, Germany). Calculations of vapor pressure of alkali oxides were performed using thermodynamic data from the software FactSage (Version 6.2).

Results

I. Powder properties

The microstructure of as-prepared KNN powder by spray pyrolysis and after calcination at 800 °C consisted of fine particles in the range 10-100 nm, as illustrated in the micrographs in Fig. 1. Some of the particles, especially the larger ones, have a characteristic cuboidal morphology. Similar size and morphology was observed for KNNLT powders (not shown). The average particle size, calculated as spherical particles from the measured surface area, increased with calcination temperature from ~100 nm at 600 °C to ~130 nm at 800 °C and ~430 nm at 1000 °C for KNN. The same trend and similar grain sizes were obtained for the KNNLT powder. The XRD patterns of KNN powders after different thermal treatments are presented in Fig. 2. A crystalline phase isostructural to $KNbO_3$ (PDF card 00-032-0822) can be observed already in the as-prepared spray pyrolyzed powder. Small amounts of a secondary phase, indexed to $K_2Nb_4O_{11}$[36] could be observed in the sintered materials. Similar trends were observed for KNNLT (not shown). Phase transitions at ~199 °C and ~412 °C for KNN and ~292 °C for KNNLT were confirmed by DSC (not shown), in agreement with previous reports.[1,14]

The particle size increased dramatically after calcination at 800 °C for the powders with excess alkali, as shown in Fig. 3. Particularly, 3 % excess K increased the average particle size by a factor of 10 compared to the stoichiometric KNN at 800 °C, and resulted in the formation of a substantial amount of cuboidal grains (Fig. 3(c)). This coarsening of the alkali excess powders was avoided by calcining the powders at 400 °C rather than 800 °C. Dispersions of KNN powders with alkali excess exhibited a higher pH (~9) compared to the stoichiometric KNN (~7) and 3 % Nb excess (~5), demonstrating the presence of a basic alkali-oxide rich phase as a consequence of the alkali excess. XRD patterns of the

stoichiometric and the non-stoichiometric KNN are presented in Fig. 4, displaying significant amounts of the secondary phase $K_2Nb_4O_{11}$ in the Nb-excess powder. This is in contrast to the alkali-excess KNN powders where no crystalline secondary phases can be observed by XRD. Secondary alkali-rich oxide phases would most likely be amorphous or X-ray amorphous due to their hygroscopic nature and reactivity with CO_2. With increasing amount of excess K the Bragg-reflections of KNN become more resolved, reflecting an increasing crystallinity or grain size. The same was observed for excess Na (not shown).

II. Densification and piezoelectric and ferroelectric properties

Dilatometry (linear shrinkage) of the nominal stoichiometric KNN and the non-stoichiometric KNN are presented in Fig. 5. Fig. 5(a) shows that densification of KNN with 3 % excess Nb appeared similar to the stoichiometric KNN. Both 3 % excess Na and K, on the other hand, exhibit a significant and sudden densification at low temperature (~650-700 °C). Fig. 5(b) displays the effect of gradual increase in the amount of excess K, similar behavior was observed for Na-excess. We observe that 2 % and 1 % excess K also resulted in a slight densification at low temperatures (~650 °C). The density of nominal stoichiometric and non-stoichiometric KNN as green ceramics and after isothermal sintering at 1100 °C is shown in Fig. 6. The highest density obtained by sintering of stoichiometric KNN (sintered at 1130 °C for 14 h in O_2) was 94 % of theoretical while for KNNLT 95 % was obtained (sintered at 1163 °C for 1 h in air). Neither alkali- nor Nb-excess improved the final density compared to the density obtained for stoichiometric KNN. Alkali excess materials prepared by calcination at 800 °C exhibited noteworthy high green densities (up to 65 %) due to dense stacking of the large, cuboidal grains, but these large cuboids also limited the densification during sintering (Fig. 3). The green density was reduced for the powders calcined at 400 °C, the lower calcination temperature was introduced to avoid coarsening and cuboidal grains. These

powders did also sinter to higher densities, although still not higher final densities than the stoichiometric KNN material calcined at 800 ºC.

The linear shrinkage during sintering of stoichiometric KNN in different atmospheres and heating rates are presented in Fig. 7. At a heating rate of 2 °C/min densification was initiated at lower temperatures and a higher final density was obtained compared to 10 °C/min. No significant differences in the densification can be observed with variation in the oxygen partial pressure. Fracture surfaces of KNN samples after dilatometry are shown in Fig. 8. A heating rate of 10 °C/min compared to 2 °C/min resulted in more uniform grain size and less exaggerated grain growth, especially for the air- and O_2-sintered samples. The grains were less cuboidal after sintering in N_2 than air and O_2, independent of heating rate. Similar results as for KNN was observed by dilatometry of the KNNLT materials. Isothermal sintering of KNN and KNNLT by direct insertion into preheated furnace (heating rate >1100 °C/min) did not improve the density compared to sintering with conventional heating rates (3.3-5 °C/min).

The polished fracture surface of 95 % dense KNNLT with cuboidal grains (average grain size 2.4 μm) presented in Fig. 9 represents the typical microstructure of the sintered ceramics with the highest densities. Piezo- and ferroelectric response of selected materials is presented in Fig. 10. The polarization loops show remnant polarization of 28.8 $\mu C/cm^2$ for KNNLT and 9.8 $\mu C/cm^2$ for KNN. Unipolar strain and normalized strain values (S_{max}/E_{max}) for KNN (147 pm/V at E_{max} = 2 kV/mm) and KNNLT (333 pm/V at E_{max} = 2 kV/mm) were within the range expected from literature.[1,13,37]

Backscatter electron micrographs of sintered and polished KNN are shown in Fig. 11. A secondary phase, often rod-shaped, was observed in most sintered KNN ceramics (Fig. 11(a)).

The cation stoichiometry of this secondary phase was found by WDS to be $(K_{1.58}Na_{0.47})Nb_4O_{11}$, corresponding to a K-rich tetragonal tungsten bronze structure ($K_2Nb_4O_{11}$), while the main phase was found to be $K_{0.42}Na_{0.58}NbO_3$. The oxygen content is estimated based on the conventional oxidation state of Na, K and Nb in KNN. Figs. 11(b)-(d) show that sintering with conventional cooling rate (3.3-5 °C/min) resulted in large secondary phase segregation compared to air-quenching.

Discussion

The spray pyrolysis yielded fine powders (small particle size and phase purity) for KNN as well as Li and Ta co-doped KNN. The high quality, combined with use of simple, inexpensive aqueous precursors and possibility of scale-up to industrial production volumes demonstrate the potential of spray pyrolysis powders as a starting point for preparation of KNN-based ceramics. The ceramics sintered from spray pyrolysis powders exhibit densities, microstructure and piezoelectric performance similar to solid-state prepared materials.[1,4,14] Despite the fine powder as a starting point, all the common challenges in processing of KNN-based ceramics cannot be avoided, and in the following the origins of these challenges with respect to the densification of KNN and related materials will be further discussed.

We observed cuboidal grains in stoichiometric KNN powders (Fig. 1), very similar to observation with KNN powders produced by other synthesis methods.[38,39] Moreover, excess alkali oxide radically increased the amount of cuboidal grains (Fig. 3(c)). As seen for alkali-excess samples in Fig. 6, the cuboidal grains easily “stack” during isostatic compression resulting in high green densities, but their lack of surface curvature removes the driving force for mass transport,[40] and further densification is limited. The rapid densification at low temperatures (650-700 °C) in alkali excess powders as observed by dilatometry (Fig. 5), can

also be rationalized by rearrangement or stacking of the cuboidal particles. We propose that this rearrangement is facilitated by a liquid phase, which is the most likely explanation for the sudden increase in the densification (Fig. 5). The liquid phase is formed from the excess alkali oxide, which we have shown by XRD and pH-measurements to exist as an X-ray amorphous phase, which makes a basic solution in contact with water. Thermodynamically one can argue that compounds with basic oxides such as alkali or alkali earth oxides will react with H_2O and CO_2 at ambient conditions. This is a well-known problem with the stability of proton conductor such as $Ba(Ce,Zr)O_3$[41] or similar Sr compounds. Possible reactions, exemplified with $KNbO_3$ instead of KNN, are shown in Eqs. (1) and (2):

$$4\ KNbO_3\ (s) + CO_2\ (g) = K_2CO_3\ (s) + K_2Nb_4O_{11}\ (s) \quad (1)$$

$$4\ KNbO_3\ (s) + H_2O\ (g) + = 2\ KOH\ (s) + K_2Nb_4O_{11}\ (s) \quad (2)$$

We therefore propose that the presence of the carbonate or hydroxide species at the surface is difficult to avoid for non-stoichiometric powders. During handling, calcination and heat treatment in air the powders are exposed to moisture and carbon dioxide which may react with the powder. The amount of alkali excess, and hence the amount of liquid phase formed, determines whether the rearrangement of the cuboidal grains can be observed macroscopically, as for 3% alkali excess (Fig. 5). For 2 and 1 % alkali excess, the amount of liquid is less than the critical amount of liquid for particle rearrangement. The formation of a low temperature liquid phase has also been discussed for alkali-rich KNN prepared by a solid state route[5,15] and $KNbO_3$ [42] powders. In these studies the liquid phase were formed at somewhat higher temperatures, but this may reflect variation in the K/Na ratio in the liquid phase.

The question one may ask is if formation of traces of alkali hydroxide or alkali carbonates at the surface of nominal stoichiometric KNN is avoidable independent on the overall cation

stoichiometry. During calcination or heat treatment of any KNN powder in ambient atmosphere, these carbonates or hydroxides will form a liquid phase promoting coarsening and particle growth in a similar manner as illustrated for the alkali excess powders in this work. This hypothesis offers an explanation of the occurrence of cuboidal grains even in stoichiometric KNN powders, and the formation of a large amount of cuboidal grains in air-sintered KNN ceramics. Higher reactivity towards CO_2 and moisture can be expected for fine grained powders as in this study and previously reported by Chowdhury *et al*.[30] This implies that KNN powders with large surface area are more susceptible to coarsening and formation of the undesired cuboidal grains, and likewise that wet chemical methods yielding fine particles are more challenging for fabrication of KNN compared to other ceramics.

Excess Nb did not give any improvement in densification compared to stoichiometric KNN (Figs. 5 and 6) which is in contrast to other works where a slight improvement has been observed,[9,15] although only when both duration and temperature of sintering were increased compared to sintering of stoichiometric KNN.[15] Nb-excess in KNN may also result as a consequence of alkali evaporation from stoichiometric KNN at high temperatures. The vapor pressure of K (g) above KNN is dependent on formation of secondary phases in the ternary system through Eq. (3) (simplified with $KNbO_3$ instead of KNN).

$$4\ KNbO_3\ (s) = 2\ K\ (g) + 1/2\ O_2\ (g) + K_2Nb_4O_{11}\ (s) \quad (3)$$

However, the vapor pressure of K (g) from this reaction cannot be calculated accurately due to lack of thermodynamic data and assumptions are necessary in order to estimate the vapor pressure. Evaporation of alkali oxides will form the elemental gas species, as shown in Eq. (4) for K_2O.

$$K_2O\ (s) = 2\ K\ (g) + ½\ O_2\ (g) \quad (4)$$

Eq. (4) constitutes a maximum estimate for the vapor pressure of K (g) over KNN. The vapor pressure of K (g) due to Eq. (4) is presented as a function of temperature and partial pressure of oxygen in Fig. 12. An estimate of the minimum of the vapor pressure of K over KNN can be calculated by Eq. (5).

$$2\ KNbO_3\ (s) = 2\ K\ (g) + ½\ O_2\ (g) + Nb_2O_5\ (s) \quad (5)$$

The vapor pressure of K (g) according to Eq. (5) is also presented in Fig. 12. The real vapor pressure falls in between these two extremes, but is most likely closer to the minimum estimate than the maximum. Considering previous work where weight loss during sintering could be detected at vapor pressures of ~10^{-6} atm,[43] the estimations of the vapor pressure suggest that evaporation of alkali and coarsening due to evaporation-condensation mechanism does only take place at the sintering temperature and not during heating to the sintering temperature, in line with the insignificant dependence of the shrinkage with respect to the partial pressure of oxygen (Fig. 7). At the sintering temperature used in this study, the presence of a $K_2Nb_4O_{11}$ type of secondary phase provides clear evidence that a reaction similar to Eq. (3) takes place.

The thermodynamic calculations demonstrate also that the vapor pressure of K (g) is higher than Na (g), in agreement with the lower melting temperature of K_2O (740 °C) compared to Na_2O (1134 °C).[44] Evaporation of Na_2O, rather than K_2O, is often said to cause alkali deficiency in sintered KNN.[23,45-49] Our calculations clearly show that K is more volatile than Na. A problem during EDS/WDS analysis is, however, misinterpretation of secondary phase grains (with lower solubility of Na than K) as matrix grains and electron beam related decomposition.[50]

Decreasing the partial pressure of oxygen during the heat treatment of KNN clearly increases the vapor pressure of alkali elements (Fig. 12) as expected from shift of the equilibria given by Eqs. (3) to (5). Higher alkali loss is therefore expected when sintered under reducing or inert conditions. This is also in agreement with the reduction of the content of cuboidal particles when sintered in inert atmosphere (Fig. 8). Recently, Kobayashi *et al.*[51] obtained high density and a uniform microstructure of KNN by sintering under reducing atmosphere ($pO_2 = 10^{-10}$ atm). How can reducing conditions improve the sintering properties of KNN when a higher alkali loss is expected from thermodynamics? We propose that the reduction of the partial pressure of oxygen also strongly destabilize residual alkali carbonate/hydroxide at the surface, as expressed for potassium carbonate and hydroxide in Eqs. (6) and (7).

$$K_2CO_3\,(l,s) = 2\,K\,(g) + \tfrac{1}{2}\,O_2\,(g) + CO_2\,(g) \qquad (6)$$

$$2KOH\,(l,s) = 2\,K\,(g) + H_2O\,(g) + \tfrac{1}{2}\,O_2\,(g)$$

Since these residual alkali carbonates/hydroxides at the surface promotes coarsening into cuboidal grains, the higher densities[51,52] and smaller and rounder grains (Fig. 8 and refs.[51,53]) observed in KNN prepared under inert/reducing conditions can be explained by evaporation of the alkali-rich excess surface layer. Reduced atmosphere will increase the evaporation of alkali oxides, but the evaporation occurs only at higher temperatures and mainly from the external surface of the sample since most of the porosity has been removed during densification. Reducing atmosphere is therefore beneficial for sintering of bulk KNN due the inhibition of the formation of cuboidal grains, but KNN thin films have been shown to be unstable in 5 % H_2/N_2 mixture even at temperatures as low as 600 °C.[54] Secondary phases due to decomposition of KNN are therefore expected at the surface of the bulk, but these can be removed by polishing in bulk specimens.

The stoichiometry of the primary and secondary phases in sintered KNN as found by WDS is in accordance with evaporation of K (g) through Eq. (3). Both the shape and the segregation of the secondary phase we observe in sintered KNN (Fig.11), similar as reported by Wang *et al.*,[55] can be rationalized by the formation of a liquid phase. This liquid phase is formed when the solidus line is crossed during sintering at high temperatures. This is not be confused with the low-temperature alkaline-rich liquid phase promoting growth of the cuboidal grains. If we consider stoichiometric KNN, the system above the solidus contains a K-rich liquid phase and a Na-rich solid phase, both on the quasi-binary $KNbO_3$-$NaNbO_3$ line.[11] However, due to evaporation of alkali (mainly K), the system is displaced to the Nb-rich side in the ternary Na_2O -K_2O-Nb_2O_5 system. Deduced from the binary K_2O-Nb_2O_5 and Na_2O-Nb_2O_5 phase diagrams[56] the solidus temperature is thereby decreased and the amount of liquid phase is increased by the alkali oxide loss. Alkali evaporation moves the overall composition out of the primary crystallization field of KNN, and the liquid phase precipitates as a mixture of KNN and $K_2Nb_4O_{11}$ during cooling. The segregation of a secondary phase (Fig. 11(b)) is hard to avoid due to the presence of a liquid phase at the sintering temperature and the complex phase equilibria during solidification of the liquid. The K/Na ratio in the liquid phase is also different from the nominal stoichiometry due the higher melting point of $NaNbO_3$, and a inhomogeneous distribution of K and Na in the sintered materials is expected as previously observed by several groups.[11,55,57] If large amounts of liquid phase are formed, more rearrangement can occur, and the secondary phase segregates into clusters during normal cooling rates (Fig. 11(c) and (d)). The presence of a liquid phase also allows for anisotropic growth of the secondary phase into a rod-shape (Fig. 11(a)) in accordance with the tetragonal tungsten bronze structure of the secondary phase.[36]

Conclusion

It was demonstrated that spray pyrolysis is a suitable method for large-scale, environmentally friendly production of KNN-based powders and apparently phase-pure $K_{0.5}Na_{0.5}NbO_3$ (KNN) and $Li_{0.03}K_{0.485}Na_{0.485}Nb_{0.8}Ta_{0.2}O_3$ (KNNLT) powders with small particle sizes were prepared (~130 nm for KNN after calcination at 800 °C). Densities above 95 % and normalized strain up to 333 pm/V were obtained by normal sintering. Alkali excess in KNN were shown to result in the formation of a liquid phase at low temperature (~650 °C), which promoted coarsening into cuboidal grains and removal of the driving force for further densification. Similarly, surface alkali-rich phases (carbonates/hydroxides) were suggested to cause coarsening into cuboidal grains even in stoichiometric KNN due to the formation of the liquid phase at the surface. The formation of this liquid phase can be avoided by low pO_2 during sintering especially during the initial stage of sintering. Neither excess Nb improved densification, but resulted in formation of $K_2Nb_4O_{11}$. This secondary phase was also formed as a consequence of alkali evaporation during sintering of stoichiometric KNN. Sintering above the solidus temperature combined with conventional cooling rates resulted in segregation of the secondary phase. Thermodynamic considerations show evaporation of K (g) to be larger than that of Na (g) and strongly dependent on pO_2 during sintering. This work shows that even with high-quality starting powders with a small particle size, the preparation of high density KNN-based piezoceramics remains challenging due to the reactivity of alkali oxides with moisture and carbon dioxide.

Acknowledgements

Financial support from NTNU and the Research Council of Norway through project number 197497/F20 «Lead-free ferro- and piezoelectric $K_{0.5}Na_{0.5}NbO_3$ -based materials» is

acknowledged. The authors would like to thank Morten Raanes for performing the WDS analyses and NTNU NanoLab for use of SEM.

References

[1]J. Rödel, W. Jo, K. T. P. Seifert, E. M. Anton, T. Granzow and D. Damjanovic, "Perspective on the Development of Lead-Free Piezoceramics," *J. Am. Ceram. Soc.*, **92** [6] 1153-77 (2009).

[2]Y. Saito, H. Takao, T. Tani, T. Nonoyama, K. Takatori, T. Homma, T. Nagaya and M. Nakamura, "Lead-Free Piezoceramics," *Nature*, **432** [7013] 84-87 (2004).

[3]B. Malic, A. Bencan, T. Rojac and M. Kosec, "Lead-Free Piezoelectrics Based on Alkaline Niobates: Synthesis, Sintering and Microstructure," *Acta Chim. Slov.*, **55** [4] 719-26 (2008).

[4]M. Kosec, B. Malic, A. Bencan and T. Rojac, "KNN-Based Piezoelectric Ceramics," pp. 81-102. in Piezoelectric and Acoustic Materials for Transducer Applications**.** Edited by A. Safari and E. K. Akdogan. Springer, New York, 2008.

[5]P. Bomlai, P. Wichianrat, S. Muensit and S. J. Milne, "Effect of Calcination Conditions and Excess Alkali Carbonate on the Phase Formation and Particle Morphology of $Na_{0.5}K_{0.5}NbO_3$ Powders," *J. Am. Ceram. Soc.*, **90** [5] 1650-55 (2007).

[6]R. L. Lehman, J. S. Gentry and N. G. Glumac, "Thermal Stability of Potassium Carbonate Near its Melting Point," *Thermochim. Acta*, **316** [1] 1-9 (1998).

[7]U. Flückiger and H. Arend, "Preparation of Pure, Doped and Reduced $KNbO_3$ Single-Crystals," *J. Cryst. Growth*, **43** [4] 406-16 (1978).

[8]A. Popovic, L. Bencze, J. Koruza, B. Malic and M. Kosec, "Knudsen Effusion Mass Spectrometric Approach to the Thermodynamics of Na_2O-Nb_2O_5 System," *Int. J. Mass Spectrom.*, **309** 70-78 (2012).

[9]M. Kosec and D. Kolar, "On Activated Sintering and Electrical Properties of $NaKNbO_3$," *Mater. Res. Bull.,* **10** [5] 335-39 (1975).

[10]J. F. Li, Y. H. Zhen, B. P. Zhang, L. M. Zhang and K. Wang, "Normal Sintering of (K, Na)NbO_3-Based Lead-Free Piezoelectric Ceramics," *Ceram. Int.,* **34** [4] 783-86 (2008).

[11]J. Fang, X. Wang, R. Zuo, Z. Tian, C. Zhong and L. Li, "Narrow Sintering Temperature Window for (K, Na)NbO_3-Based Lead-Free Piezoceramics Caused by Compositional Segregation," *Phys. Status Solidi A,* **208** [4] 791-94 (2011).

[12]R. Jaeger and L. Egerton, "Hot Pressing of Potassium-Sodium Niobates," *J. Am. Ceram. Soc.,* **45** [5] 209-13 (1962).

[13]H. Y. Park, J. Y. Choi, M. K. Choi, K. H. Cho, S. Nahm, H. G. Lee and H. W. Kang, "Effect of CuO on the Sintering Temperature and Piezoelectric Properties of $(Na_{0.5}K_{0.5})NbO_3$ Lead-Free Piezoelectric Ceramics," *J. Am. Ceram. Soc.,* **91** [7] 2374-77 (2008).

[14]E. Hollenstein, M. Davis, D. Damjanovic and N. Setter, "Piezoelectric Properties of Li- and Ta-Modified $(K_{0.5}Na_{0.5})NbO_3$ Ceramics," *Appl. Phys. Lett.,* **87** [18] 182905-7 (2005).

[15]J. Acker, H. Kungl and M. J. Hoffmann, "Influence of Alkaline and Niobium Excess on Sintering and Microstructure of Sodium-Potassium Niobate $(K_{0.5}Na_{0.5})NbO_3$," *J. Am. Ceram. Soc.,* **93** [5] 1270-81 (2010).

[16]N. M. Hagh, B. Jadidian and A. Safari, "Property-Processing Relationship in Lead-Free (K, Na, Li) NbO_3-Solid Solution System," *J. Electroceram.,* **18** [3-4] 339-46 (2007).

[17]J. G. Fisher, D. Rout, K. S. Moon and S. J. L. Kang, "Structural Changes in Potassium Sodium Niobate Ceramics Sintered in Different Atmospheres," *J. Alloy. Compd.,* **479** [1-2] 467-72 (2009).

[18]T. Rojac, A. Bencan, H. Ursic, B. Malic and M. Kosec, "Synthesis of a Li- and Ta-Modified (K,Na)NbO_3 Solid Solution by Mechanochemical Activation," *J. Am. Ceram. Soc.*, **91** [11] 3789-91 (2008).

[19]A. Reisman and F. Holtzberg, "Phase Equilibria in the System K_2CO_3-Nb_2O_5 by the Method of Differential Thermal Analysis," *J. Am. Chem. Soc.*, **77** [8] 2115-19 (1955).

[20]L. Egerton and D. Dillon, "Piezoelectric and Dielectric Properties of Ceramics in the System Potassium Sodium Niobate," *J. Am. Ceram. Soc.*, **42** [9] 438-42 (1959).

[21]Z. S. Z. Ahn, "Conventionally Sintered ($Na_{0.5}$,$K_{0.5}$)NbO_3 with Barium Additions," *J. Am. Ceram. Soc.*, **70** [1] 18-21 (1987).

[22]K.-I. Kakimoto, Y. Hayakawa and I. Kagomiya, "Low-Temperature Sintering of Dense (Na,K)NbO_3 Piezoelectric Ceramics Using the Citrate Precursor Technique," *J. Am. Ceram. Soc.*, **93** [9] 2423-26 (2010).

[23]Y. Wang, D. Damjanovic, N. Klein, E. Hollenstein and N. Setter, "Compositional Inhomogeneity in Li- and Ta-Modified (K, Na)NbO_3 Ceramics," *J. Am. Ceram. Soc.*, **90** [11] 3485-89 (2007).

[24]M. I. Morozov, M. J. Hoffmann, K. Benkert and C. Schuh, "Influence of the A/B Nonstoichiometry, Composition Modifiers, and Preparation Methods on Properties of Li- and Ta-Modified (K,Na)NbO_3 Ceramics," *J. Appl. Phys.*, **112** [11] 114107-9 (2012).

[25]F. Zhang, L. Han, S. Bai, T. D. Sun, T. Karaki and M. Adachi, "Hydrothermal Synthesis of (K,Na)NbO_3 Particles," *Jpn. J. Appl. Phys.*, **47** [9] 7685-88 (2008).

[26]L. Bai, K. Zhu, L. Su, J. Qiu and H. Ji, "Synthesis of (K, Na)NbO_3 Particles by High Temperature Mixing Method under Hydrothermal Conditions," *Materials Letters*, **64** [1] 77-79 (2010).

[27]R. Lopez, F. Gonzalez, M. P. Cruz and M. E. Villafuerte-Castrejon, "Piezoelectric and Ferroelectric Properties of $K_{0.5)}Na_{0.5}NbO_3$ Ceramics Synthesized by Spray Drying Method," *Mater. Res. Bull.,* **46** [1] 70-74 (2011).

[28]R. Lopez, F. Gonzalez and M. E. Villafuerte-Castrejon, "Structural and Electrical Characterization of $(K_{0.48}Na_{0.52})_{0.96}Li_{0.04}Nb_{0.85}Ta_{0.15}O_3$ Synthesized by Spray Drying," *J. Eur. Chem. Soc.,* **30** [6] 1549-53 (2010).

[29]K. Tanaka, H. Hayashi, K.-i. Kakimoto, H. Ohsato and T. Iijima, "Effect of (Na,K)-Excess Precursor Solutions on Alkoxy-Derived (Na,K)NbO_3 Powders and Thin Films," *Jpn. J. Appl. Phys. Part 1 - Regul. Pap. Brief Commun. Rev. Pap.,* **46** [10B] 6964-70 (2007).

[30]A. Chowdhury, S. O'Callaghan, T. A. Skidmore, C. James and S. J. Milne, "Nanopowders of $Na_{0.5}K_{0.5}NbO_3$ Prepared by the Pechini Method," *J. Am. Ceram. Soc.,* **92** [3] 758-61 (2009).

[31]G. L. Messing, S. C. Zhang and G. V. Jayanthi, "Ceramic Powder Synthesis by Spray Pyrolysis," *J. Am. Ceram. Soc.,* **76** [11] 2707-26 (1993).

[32]D. Segal, "Chemical Synthesis of Ceramic Materials," *J. Mater. Chem.,* **7** [8] 1297-305 (1997).

[33]Ø. F. Lohne, J. Gurauskis, T. N. Phung, M.-A. Einarsrud, T. Grande, H. J. M. Bouwmeester and K. Wiik, "Effect of B-Site Substitution on the Stability of $La_{0.2}Sr_{0.8}Fe_{0.8}B_{0.2}O_{3-\delta}$, B = Al, Ga, Cr, Ti, Ta, Nb," *Solid State Ion.,* **225** [0] 186-89 (2012).

[34]V. Gil, R. A. Strøm, L. J. Groven and M.-A. Einarsrud, "$La_{28-x}W_{4+x}O_{54+3x/2}$ Powders Prepared by Spray Pyrolysis," *J. Am. Ceram. Soc.,* **95** [11] 3403-07 (2012).

[35]A. B. Haugen, I. Kumakiri, C. Simon and M. A. Einarsrud, "TiO_2, TiO_2/Ag and TiO_2/Au Photocatalysts Prepared by Spray Pyrolysis," *J. Eur. Chem. Soc.,* **31** [3] 291-98 (2011).

[36]F. Madaro, R. Sæterli, J. R. Tolchard, M.-A. Einarsrud, R. Holmestad and T. Grande, "Molten Salt Synthesis of $K_4Nb_6O_{17}$, $K_2Nb_4O_{11}$ and KNb_3O_8 Crystals with Needle- or Plate-Like Morphology," *Crystengcomm,* **13** [5] 1304-13 (2011).

[37]Y. Saito and H. Takao, "High Performance Lead-Free Piezoelectric Ceramics in the $(K,Na)NbO_3$-$LiTaO_3$ Solid Solution System," *Ferroelectrics,* **338** 1433-48 (2006).

[38]G. Stavber, B. Mali and M. Kosec, "A Road to Environmentally Friendly Materials Chemistry: Low-Temperature Synthesis of Nanosized $K_{0.5}Na_{0.5}NbO_3$ Powders Through Peroxide Intermediates in Water," *Green Chem.*, **13** [5] 1303-10 (2011).

[39]E. Ringgaard and T. Wurlitzer, "Lead-Free Piezoceramics Based on Alkali Niobates," *J. Eur. Chem. Soc.*, **25** [12] 2701-06 (2005).

[40]R. M. German, "Sintering Theory and Practice." John Wiley & Sons: New York, 1996.

[41]A. Eriksson, M.-A. Einarsrud and T. Grande, "Materials Science Aspects Relevant for High-Temperature Electrochemistry," pp. 415-65. in Solid State Electrochemistry II**.** Edited by V. V. Kharton. Wiley-VCH, Weinheim, Germany, 2011.

[42]J. Acker, H. Kungl and M. J. Hoffmann, "Sintering and Microstructure of Potassium Niobate Ceramics with Stoichiometric Composition and with Potassium- or Niobium Excess," *J. Eur. Chem. Soc.*, **33** [11] 2127-39 (2013).

[43]T. Grande, H. Sommerset, E. Hagen, K. Wiik and M.-A. Einarsrud, "Effect of Weight Loss on Liquid-Phase-Sintered Silicon Carbide," *J. Am. Ceram. Soc.*, **80** [4] 1047-52 (1997).

[44]"CRC Handbook of Chemistry and Physics," **Vol. 94**. Taylor and Francis Group, http://www.hbcpnetbase.com 2013.

[45]Y. Zhen, "Normal Sintering of $(K,Na)NbO_3$-Based Ceramics: Influence of Sintering Temperature on Densification, Microstructure, and Electrical Properties," *J. Am. Ceram. Soc.*, **89** [12] 3669-75 (2006).

[46]H. C. Song, K. H. Cho, H. Y. Park, C. W. Ahn, S. Nahm, K. Uchino and S. H. Park, "Microstructure and Piezoelectric Properties of (1-x)($Na_{0.5}K_{0.5}$)NbO_3-x$LiNbO_3$ Ceramics," *J. Am. Ceram. Soc.*, **90** [6] 1812-16 (2007).

[47]C.-W. Ahn, C.-S. Park, C.-H. Choi, S. Nahm, M.-J. Yoo, H.-G. Lee and S. Priya, "Sintering Behavior of Lead-Free (K,Na)NbO_3-Based Piezoelectric Ceramics," *J. Am. Ceram. Soc.*, **92** [9] 2033-38 (2009).

[48]K.-H. Cho, H.-Y. Park, C.-W. Ahn, S. Nahm, K. Uchino, S.-H. Park, H.-G. Lee and H.-J. Lee, "Microstructure and Piezoelectric Properties of 0.95($Na_{0.5}K_{0.5}$)NbO_3–0.05$SrTiO_3$ Ceramics," *J. Am. Ceram. Soc.*, **90** [6] 1946-49 (2007).

[49]C.-W. Ahn, H.-Y. Park, S. Nahm, K. Uchino, H.-G. Lee and H.-J. Lee, "Structural Variation and Piezoelectric Properties of 0.95($Na_{0.5}K_{0.5}$)NbO_3–0.05$BaTiO_3$ Ceramics," *Sensor. Actuat. A-Phys.*, **136** [1] 255-60 (2007).

[50]S. Sturm, A. Bencan, M. A. Gulgun, B. Malic and M. Kosec, "Determining the Stoichiometry of (K,Na)NbO_3 Using Optimized Energy-Dispersive X-Ray Spectroscopy and Electron Energy-Loss Spectroscopy Analyses in a Transmission Electron Microscope," *J. Am. Ceram. Soc.*, **94** [8] 2633-39 (2011).

[51]K. Kobayashi, Y. Doshida, Y. Mizuno and C. A. Randall, "A Route Forwards to Narrow the Performance Gap between PZT and Lead-Free Piezoelectric Ceramic with Low Oxygen Partial Pressure Processed ($Na_{0.5}K_{0.5}$)NbO_3," *J. Am. Ceram. Soc.*, **95** [9] 2928-33 (2012).

[52]J. G. Fisher, D. Rout, K.-S. Moon and S.-J. L. Kang, "High-Temperature X-Ray Diffraction and Raman Spectroscopy Study of ($K_{0.5}Na_{0.5}$)NbO_3 Ceramics Sintered in Oxidizing and Reducing Atmospheres," *Mater. Chem. Phys.*, **120** [2-3] 263-71 (2010).

[53]J. G. Fisher and S.-J. L. Kang, "Microstructural Changes in ($K_{0.5}Na_{0.5}$)NbO_3 Ceramics Sintered in Various Atmospheres," *J. Eur. Chem. Soc.*, **29** [12] 2581-88 (2009).

[54]K.-N. Pham, T. Grande and M.-A. Einarsrud, *Unpublished work.*

[55]Y. L. Wang, D. Damjanovic, N. Klein and N. Setter, "High-Temperature Instability of Li- and Ta-Modified (K,Na)NbO_3 Piezoceramics," *J. Am. Ceram. Soc.,* **91** [6] 1962-70 (2008).

[56]E. Irle, R. Blachnik and B. Gather, "The Phase Diagrams of Na_2O and K_2O with Nb_2O_5 and the Ternary System Nb_2O_5-Na_2O-Yb_2O_3," *Thermochim. Acta,* **179** [1] 157-69 (1991).

[57]S. J. Zhang, H. J. Lee, C. Ma and X. L. Tan, "Sintering Effect on Microstructure and Properties of (K,Na)NbO_3 Ceramics," *J. Am. Ceram. Soc.,* **94** [11] 3659-65 (2011).

Figure captions

Fig 1. (a) As-prepared spray pyrolyzed KNN powder (dry milled to improve view of particles) and (b) KNN powder calcined at 800 °C and milled.

Fig. 2. XRD patterns of as-prepared KNN powder, after calcination at 800 °C and after sintering at 1130 °C. All patterns have been normalized on their most intense reflection.

Fig. 3. (a) Average particle size of KNN and KNN with excess alkali (K or Na) after calcination at the indicated temperature. The error bars are smaller than the size of the symbols, (b) micrograph of 3 % excess K calcined at 400 °C and (c) micrograph of 3 % excess K calcined at 800 °C.

Fig. 4. XRD of KNN and non-stoichiometric KNN after sintering at 1100 °C (1130 °C for KNN). All patterns have been normalized on their most intense reflection. * Indicates secondary phase indexed to $K_2Nb_4O_{11}$.

Fig. 5. Linear shrinkage and shrinkage rate (inset) of (a) stoichiometric KNN and KNN with 3 % excess K, Na and Nb, and (b) stoichiometric KNN and KNN with 1-3 % K-excess. Alkali excess powders were calcined at 400 °C, KNN and 3 % Nb at 800 °C.

Fig. 6. Density of green bodies and sintered KNN, stoichiometric and with excess K or Nb, calcination temperature is indicated. Included is also the highest density obtained by sintering of stoichiometric KNN (sintered at 1130 °C for 14 h in O_2) and KNNLT (sintered at 1163 °C for 1 h in air).

Fig. 7. Dilatometry curves of stoichiometric KNN in N_2, air and O_2 at heating rates 2 and 10 C/min.

Fig. 8. Fracture surfaces of stoichiometric KNN after dilatometry studies in different atmospheres and heating rates. (a) 2 °C /min in N_2,(b) 10 °C /min in N_2, (c) °C /min in air, (d) 10 °C/min in air,(e) 2 °C /min in O_2, and (f) 10 °C /min in O_2.

Fig. 9. Microstructure of polished and thermally etched fracture surface of KNNLT (95 % dense) sintered at 1156° C for 1 h.

Fig. 10. (a) Polarization hysteresis loops of KNN (94 % dense) and KNNLT (92 % dense) and (b) unipolar strain curves for KNN and KNNLT.

Fig. 11. Backscatter electron micrographs of polished cross sections of nominally stoichiometric KNN showing secondary phase (bright areas). (a) KNN sample sintering at 1145 °C for 1 h by direct insertion into preheated furnace and air-quenched, (b-c) distribution of the secondary phase: (b) same sample as in (a), (c) KNN sintered for 1 h at 1150 °C (heating and cooling rates 3.3 °C/min), and (d) KNN sintered for 14 h at 1130 °C (in O_2) (heating and cooling rates 5 °C/min).

Fig. 12. Calculated vapor pressures of K and Na vs. temperature. For K, both vapor pressures according to equations for maximum (Eq. (4)) and minimum (Eq. (5)) evaporation are presented, for a selection of partial pressures of oxygen. For Na only the maximum evaporation in air is presented.

Figures

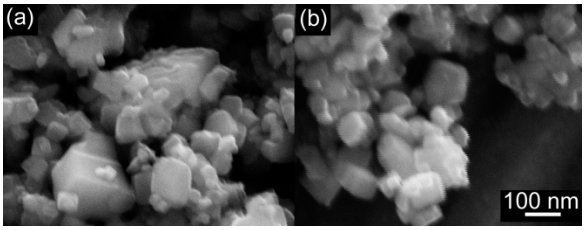

Fig 1. (a) As-prepared spray pyrolyzed KNN powder (dry milled to improve view of particles) and (b) KNN powder calcined at 800 °C and milled.

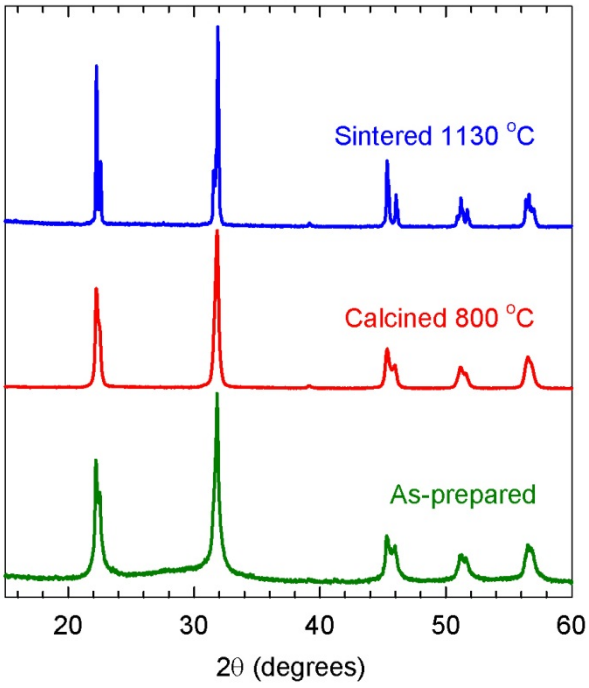

Fig. 2. XRD patterns of as-prepared KNN powder, after calcination at 800 °C and after sintering at 1130 °C. All patterns have been normalized on their most intense reflection.

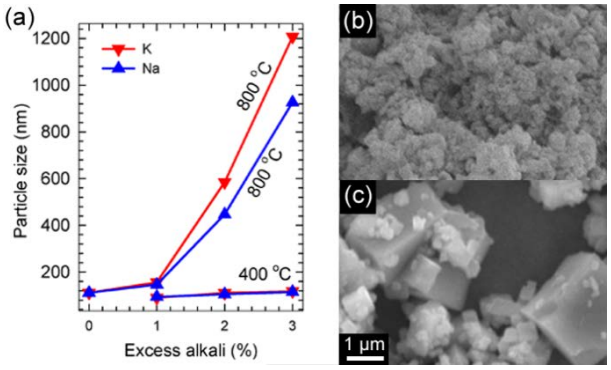

Fig. 3. (a) Average particle size of KNN and KNN with excess alkali (K or Na) after calcination at the indicated temperature. The error bars are smaller than the size of the symbols, (b) micrograph of 3 % excess K calcined at 400 °C and (c) micrograph of 3 % excess K calcined at 800 °C.

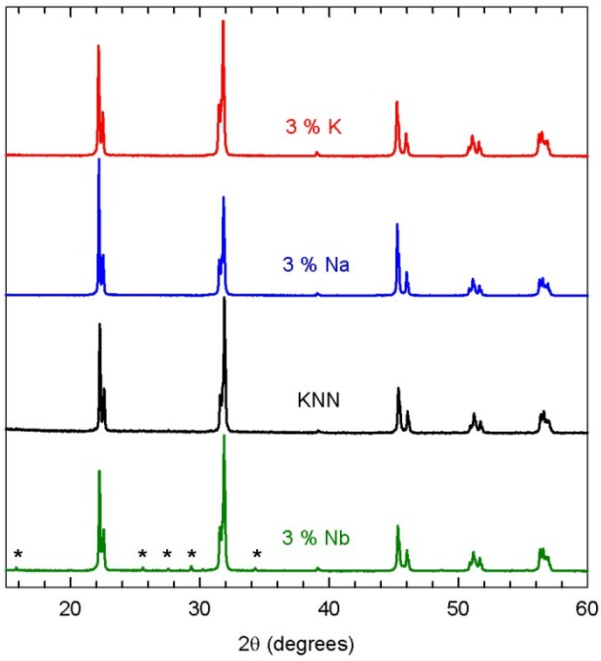

Fig. 4. XRD of KNN and non-stoichiometric KNN after sintering at 1100 °C (1130 °C for KNN). All patterns have been normalized on their most intense reflection. * Indicates secondary phase indexed to $K_2Nb_4O_{11}$.

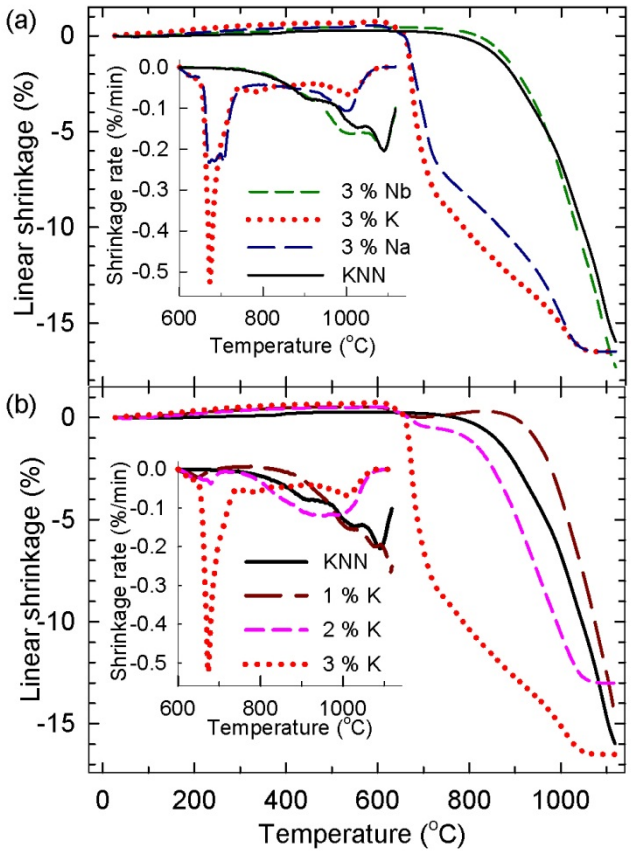

Fig. 5. Linear shrinkage and shrinkage rate (inset) of (a) stoichiometric KNN and KNN with 3 % excess K, Na and Nb, and (b) stoichiometric KNN and KNN with 1-3 % K-excess. Alkali excess powders were calcined at 400 °C, KNN and 3 % Nb at 800 °C.

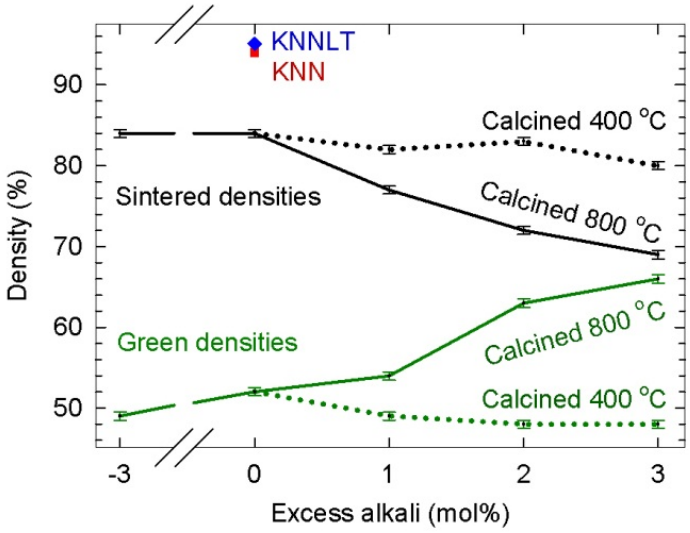

Fig. 6. Density of green bodies and sintered KNN, stoichiometric and with excess K or Nb, calcination temperature is indicated. Included is also the highest density obtained by sintering of stoichiometric KNN (sintered at 1130 °C for 14 h in O_2) and KNNLT (sintered at 1163 °C for 1 h in air).

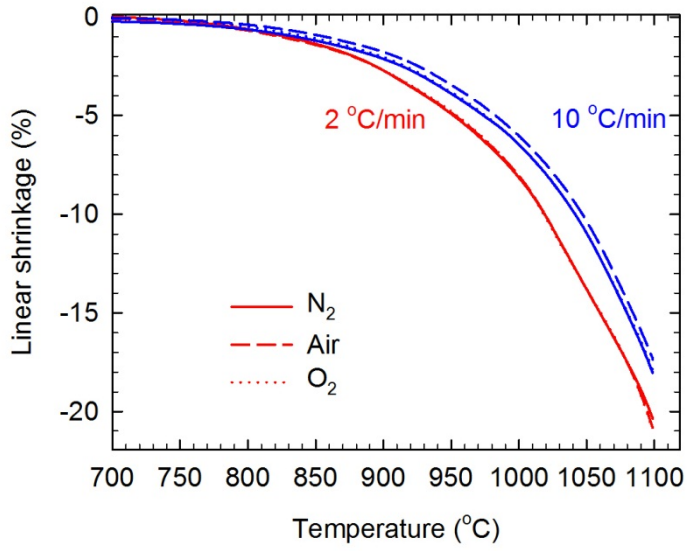

Fig. 7. Dilatometry curves of stoichiometric KNN in N_2, air and O_2 at heating rates 2 and 10 C/min.

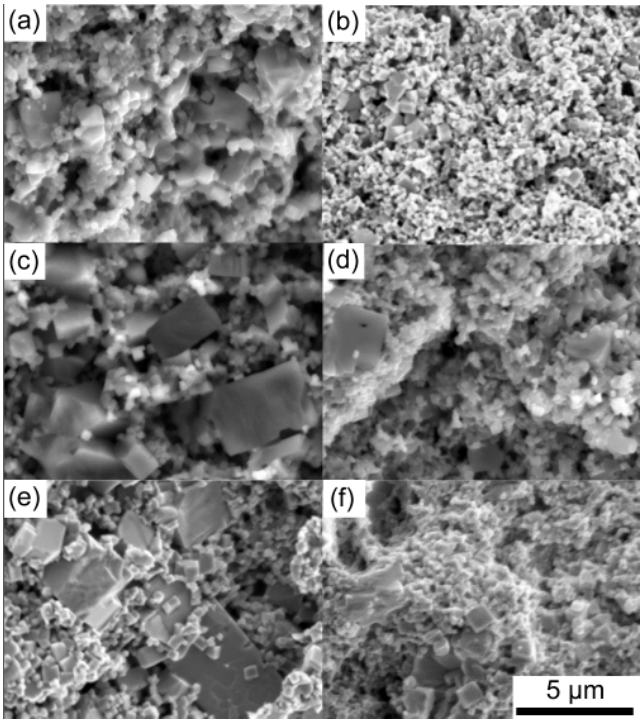

Fig. 8. Fracture surfaces of stoichiometric KNN after dilatometry studies in different atmospheres and heating rates. (a) 2 °C /min in N_2, (b) 10 °C /min in N_2, (c) °C /min in air, (d) 10 °C/min in air, (e) 2 °C /min in O_2, and (f) 10 °C /min in O_2.

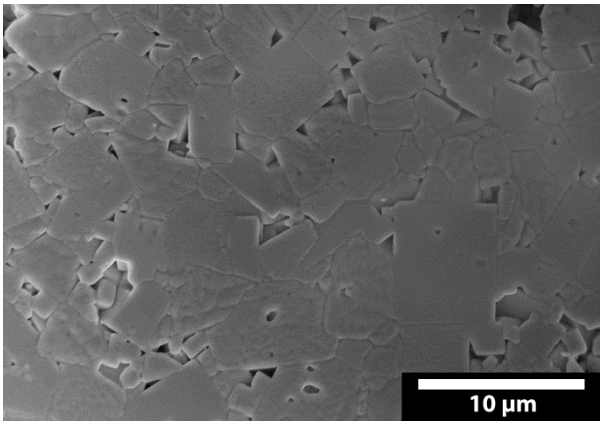

Fig. 9. Microstructure of polished and thermally etched fracture surface of KNNLT (95 % dense) sintered at 1156° C for 1 h.

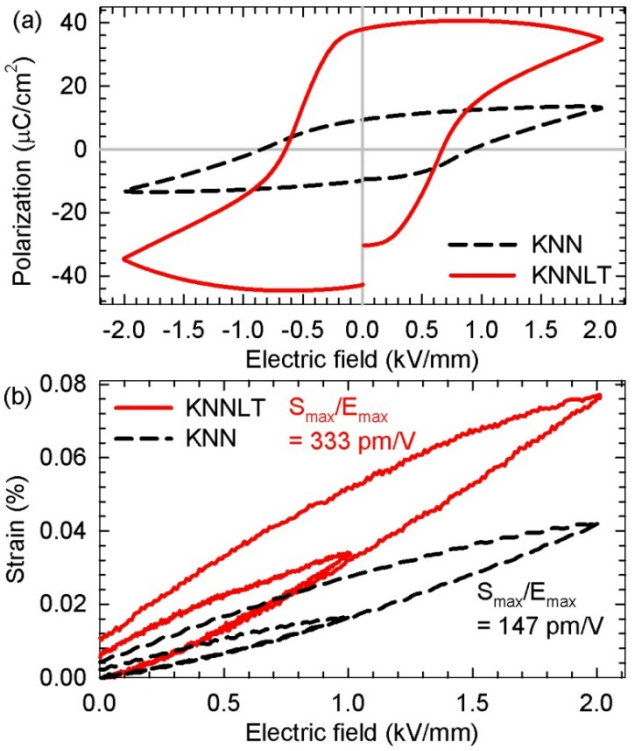

Fig. 10. (a) Polarization hysteresis loops of KNN (94 % dense) and KNNLT (92 % dense) and (b) unipolar strain curves for KNN and KNNLT.

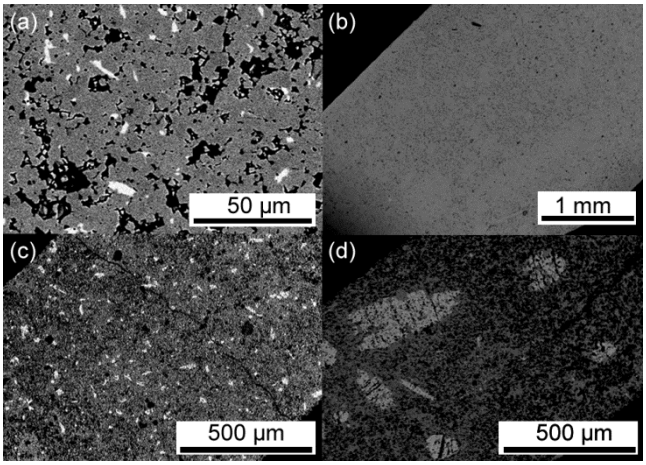

Fig. 11. Backscatter electron micrographs of polished cross sections of nominally stoichiometric KNN showing secondary phase (bright areas). (a) KNN sample sintering at 1145 °C for 1 h by direct insertion into preheated furnace and air-quenched, (b-c) distribution of the secondary phase: (b) same sample as in (a), (c) KNN sintered for 1 h at 1150 °C (heating and cooling rates 3.3 °C/min), and (d) KNN sintered for 14 h at 1130 °C (in O_2) (heating and cooling rates 5 °C/min).

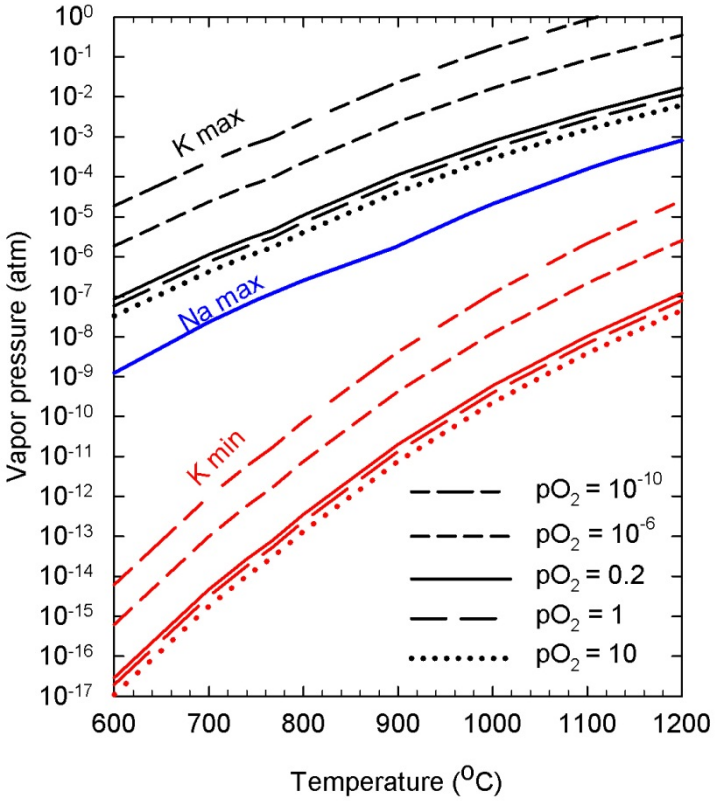

Fig. 12. Calculated vapor pressures of K and Na vs. temperature. For K, both vapor pressures according to equations for maximum (Eq. (4)) and minimum (Eq. (5)) evaporation are presented, for a selection of partial pressures of oxygen. For Na only the maximum evaporation in air is presented.